Journal of Ginseng Research 48 (2024) 236–244

Contents lists available at ScienceDirect

Journal of Ginseng Research

journal homepage: www.sciencedirect.com/journal/journal-of-ginseng-research

Research Article

Foeniculum vulgare essential oil nanoemulsion inhibits *Fusarium oxysporum* causing *Panax notoginseng* root-rot disease

Hongyan Nie, Hongxin Liao, Jinrui Wen, Cuiqiong Ling, Liyan Zhang, Furong Xu, Xian Dong *

School of Chinese Materia Medica, Yunnan University of Chinese Medicine, Kunming, China

ARTICLE INFO

Keywords:
Natural product
Nanoemulsion
Antifungal mechanism
Transcriptome
Metabolome

ABSTRACT

Background: *Fusarium oxysporum* (*F. oxysporum*) is the primary pathogenic fungus that causes *Panax notoginseng* (*P. notoginseng*) root rot disease. To control the disease, safe and efficient antifungal pesticides must currently be developed.

Methods: In this study, we prepared and characterized a nanoemulsion of *Foeniculum vulgare* essential oil (Ne-FvEO) using ultrasonic technology and evaluated its stability. Traditional *Foeniculum vulgare* essential oil (T-FvEO) was prepared simultaneously with 1/1000 Tween-80 and 20/1000 dimethyl sulfoxide (DMSO). The effects and inhibitory mechanism of Ne-FvEO and T-FvEO in *F. oxysporum* were investigated through combined transcriptome and metabolome analyses.

Results: Results showed that the minimum inhibitory concentration (MIC) of Ne-FvEO decreased from 3.65 mg/mL to 0.35 mg/mL, and its bioavailability increased by 10-fold. The results of gas chromatography/mass spectrometry (GC/MS) showed that T-FvEO did not contain a high content of estragole compared to *Foeniculum vulgare* essential oil (FvEO) and Ne-FvEO. Combined metabolome and transcriptome analysis showed that both emulsions inhibited the growth and development of *F. oxysporum* through the synthesis of the cell wall and cell membrane, energy metabolism, and genetic information of *F. oxysporum* mycelium. Ne-FvEO also inhibited the expression of 2-oxoglutarate dehydrogenase and isocitrate dehydrogenase and reduced the content of 2-oxoglutarate, which inhibited the germination of spores.

Conclusion: Our findings suggest that Ne-FvEO effectively inhibited the growth of *F. oxysporum* in *P. notoginseng* in vivo. The findings contribute to our comprehension of the antifungal mechanism of essential oils (EOs) and lay the groundwork for the creation of plant-derived antifungal medicines.

1. Introduction

The root of *Panax notoginseng* (Burk.) F.H. Chen (*P. notoginseng*), commonly known as Tianqi, is a highly valuable traditional Chinese medicine that is predominantly found in Yunnan and Guangxi provinces [1]. The main ingredient of *P. notoginseng* is *P. notoginseng* saponins (PNSs), which have many beneficial effects on the cardiovascular, lung, and central neurological systems [2]. It can be seen P. notoginseng has high medicinal value. However, P. notoginseng is prone to a variety of plant diseases, among which root rot is the most serious, and *Fusarium oxysporum* (*F. oxysporum*) is one of the main pathogens causing root rot [3]. *F. oxysporum* can survive in soil for decades by producing chlamydospores. When the spores are stimulated by root secretions, they germinate and infect the root system, causing a new round of disease. Therefore, management of *Fusarium* root rot is a challenging task [4].

Some chemical pesticides are currently used to control *P. notoginseng* root rot, however, overusing chemical pesticides can easily result in a number of issues, including excessive pesticide residues and heightened pathogen resistance. It is no longer practical to control *P. notoginseng* roots with typical chemical treatments. Therefore, it is urgent to find a low toxicity, high efficiency and no residual fungicide. EOs are volatile aromatic extracts from plant materials and are generally recognized as safe (GRAS) by the FDA [5,6]. Numerous investigations have demonstrated that EOs have potent antifungal properties [7,8], each essential oil (EO) has between 20 and 80 unique chemical types [9,10]. *Foeniculum vulgare* (*F. vulgare*), a member of the *Apiaceae* family, is a significant medicinal plant that may be found practically everywhere in the world [5]. Its seed extract has antifungal effects against *Aspergillus flavus* sp., *Candida albicans* sp., *Sclerotinia sclerotiorum* and many other phytopathogens and dermatophytes [4,11]. Scientific proof shows that

* Corresponding author. School of Chinese Materia Medica, Yunnan University of Chinese Medicine, Kunming, China.
E-mail address: dongxian_1655129@163.com (X. Dong).

https://doi.org/10.1016/j.jgr.2023.12.002
Received 3 August 2023; Received in revised form 12 December 2023; Accepted 13 December 2023
Available online 20 December 2023

F. vulgare essential oils (EOs) can prevent the accumulation of microorganisms [12,13]. However, the volatility, low water solubility, low stability, and low bioavailability of EOs restrict their development and use. Due to their smaller particle size, regulated release characteristics, and stability compared to the free form, nanoencapsulated EOs have been shown to have higher antifungal and antimycotoxigenic activity [14,15]. Therefore, it is anticipated that EOs and their nanoencapsulated compositions will be an efficient way to reduce the danger of mycotoxin and fungus infection in the cultivation of Chinese herbal remedies. Since the antifungal mechanism of EOs has not been fully studied, the development of new green pesticides or antifungal drugs is difficult and blind. In order to further investigate the antifungal mechanism of EOs against fungal growth, Yang et al. [16] prepared O/W (oil/water) nanoemulsions of eugenol, carvacrol and cinnamaldehyde using high-pressure microjets. The nanoemulsion reduced *Penicillium digitatum* spore germination and changed the permeability of cell membrane. Compared to free *Myristica fragrans* EO, nanoemulsions exhibit greater antifungal, antimycotoxic, and antioxidant properties [17]. A growing number of studies indicate that EOs and nanoencapsulated EOs has potential antifungal activity.

In this study, the physiological indicators of *F. oxysporum* were used to evaluate the inhibitory effect of EO, and transcriptomic and metabolomic analysis were combined to reveal its mechanism of action. Based on the results of this study, it is expected to find the antifungal target of EOs, and provide a theoretical basis for the preparation of environmentally friendly pesticides to control the root rot of medicinal plants.

2. Materials and methods

2.1. Plants and fungal strain

P. notoginseng seeds were supplied by Yunnan Wenshan Jinyuan Agricultural Development Co., Ltd. They were sown in a 4:1 nutritious soil: clay matrix and cultured at 65 % ± 5 % relative humidity, 14 h/d photoperiod, and 20 °C till germination.

The isolates of *P. notoginseng* root rot were inoculated on PDA medium for culture. After DNA extraction, and target genes were sequenced and identified using the fungal internal transcriptional spacer (ITS). The primers were ITS1, 5′-TCCGTAGAGAACCTGG-3′ and ITS4, 5′-TCCTCGCTTATGC-3’. Sequencing was completed by China Shengong Biotechnology Co., Ltd., and the sequencing results were uploaded to GenBank. BLAST analysis revealed that these sequences were homologous to *F. oxysporum*, and the homology was 100 %. The accession number in GenBank is OQ080022.1.

2.2. Preparation of FvEO and T-FvEO

F. vulgare seeds were purchased from the Yunnan Deyang Yuanzhi Medicine Business Department (Kunming, Yun-nan Province). *F. vulgare* seeds were mixed with distilled water in a 10 L round bottom flask and steam distillation was used to extract EO. Anhydrous sodium sulfate was added to the collected EO to eliminate excess water and stored in sealed brown vials at −20 °C until use. FvEO was dissolved in 2-DMSO-T (aqueous solution of 2 % DMSO and 0.1 % Tween 80), after which it was ultrasonically processed in an ice bath for 20 min.

2.3. The optimal Ne-FvEO formulation is prepared by choosing the mass ratio of the cosurfactant and surfactant (Km value)

The Km values were determined by the pseudoternary phase diagram method based on the selected surfactant (Tween 80) and cosurfactant (anhydrous ethanol). At room temperature, the solution with a Km value of 2:1 (Tween 80: anhydrous ethanol = 2:1) was weighed and stirred for 10 min. The primary crude emulsion was treated by ultrasonic homogenizer (Ningbo Xinzhi Biotechnology Co., Ltd, China) for 30 min under the condition of 600 W working power and 40 kHz in ice water bath. After sealing, Km and FvEO were mixed at a mass ratio of 8:2 (total mass 5 g) and stirred for 5 min. After adding 4 g of distilled water, the emulsion was clear and transparent. Ultrasonic treatment in ice bath for 30 min yielded Ne-FvEO.

2.4. Morphological observation and particle size analysis of T-FvEO and Ne-FvEO

According to related literature [17], Ne-FvEO was diluted with distilled water 10 times and studied by transmission electron microscopy (TEM) (JEM-1011, JEOL, Co. Ltd., Tokyo, Japan). The particle size distribution of nanoemulsion was measured through Laser particle size analyzer (90 Plus PALS).

2.5. Stability experiments of Ne-FvEO

Ne-FvEO was centrifuged for 30 min at 2000, 5000 and 8000 rpm for stability analysis. Subsequently, stability was tested at room temperature (24.3 °C), refrigerator temperatures (−20 °C and 4 °C), 25 °C, 30 °C, 35 °C and 40 °C. Stability tests were also performed at pH = 5, 6, 8 and 9 and at salt concentrations of 1 %, 3 % and 5 %. Then, Ne-FvEO was diluted to 25 mg/mL with distilled water and placed under different light intensities (0, 30 %, 60 %, 90 %) for 48 h to compare whether there was a change in antifungal activity.

2.6. Antifungal activity measurements

2.6.1. Determination of MIC

According to the method outlined by Balouiri M et al. [18], the diluted EOs were filtered using a 0.22 μm Millipore filter. The concentration of the prepared spore suspension was adjusted to 1×10^5 spores mL^{-1}. The initial concentration of Ne-FvEO and Ne-FvEO were 5 mg/mL and 25 mg/mL, respectively. By using double dilution, eight concentration gradients were created from two emulsions. 96-well plates were incubated at 28°Cfor 20 h. The MIC of the emulsion was calculated by measuring the absorbance of each well with a microplate reader at 595 nm.

2.6.2. Mycelial growth test

The mycelial growth test was carried out according to the method described by Sindhu et al. [19] with slight modification. Different concentrations of Ne-FvEO and T-FvEO were added to the medium, quickly shaken and poured into the PDA medium. An *F. oxysporum* mycelial disc (8 mm diameter) was placed on PDA medium at the center of the Petri plate. Parafilm-sealed petri plates were darkly incubated at 28 °C for 5 days. Colony diameter was mesured by calipers.

2.6.3. Spore germination test

Spore germination inhibition was analyzed according to Xu et al. [20] with minor modifications. Different concentrations of Ne-FvEO and T-FvEO were added to *F. oxysporum* spore suspension, respectively. After being stored at 28 °C for 12 h, the spore germination was tracked under a microscope. Germination inhibition rate formula: germination inhibition rate (%) = [(Ac–Al)/Ac] × 100, where Ac is the control germination rate and Al is the germination rate after treatment with Ne-FvEO or T-FvEO.

2.7. Composition analysis by GC–MS of Ne-FvEO and T-FvEO

The chemical compositions of FvEO, Ne-FvEO and T-FvEO were determined by GC–MS (Agilent Technologies 7890 B–5977 B, Beijing, China). The retention time and mass spectra of compounds were compared with the NIST 17. L database and the final chemical constituents were determined with relevant literature [21].

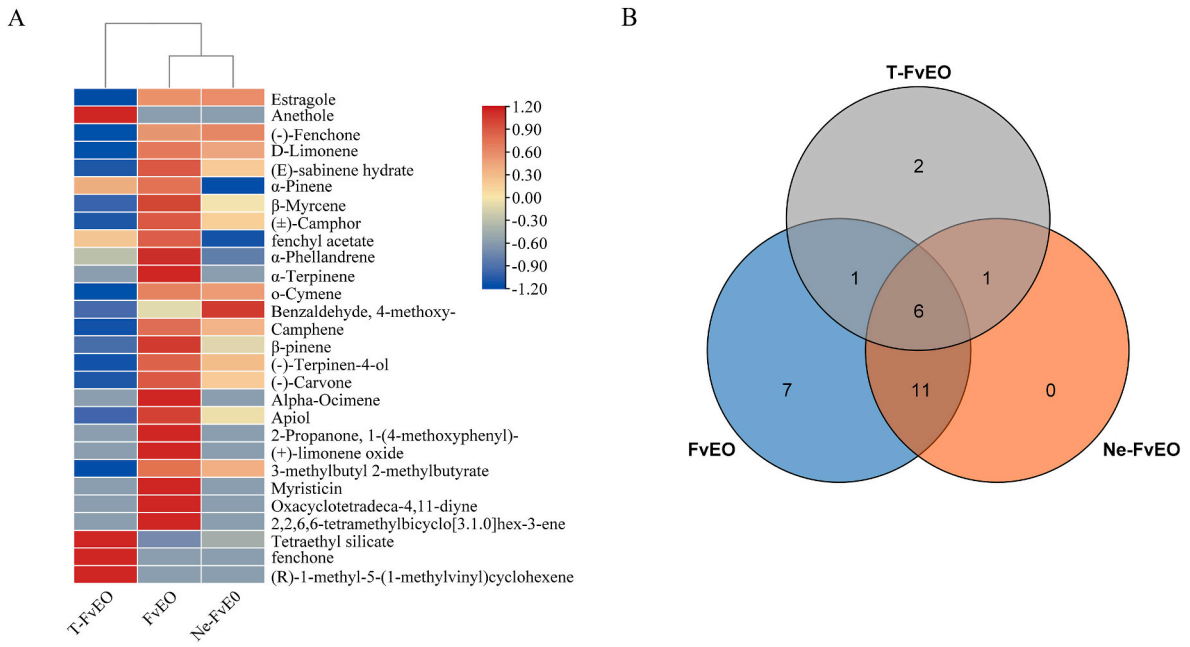

Fig. 1. Cluster heatmaps and Venn diagrams of the chemical constituents of FvEO, Ne-FvEO and T-FvEO. (A) The base logarithmic scale of the GC–MS peak area was used for the cluster heatmaps of the three groups. (B) Venn diagram of major chemical components.

2.8. Transcriptomic and metabolomic analysis

F. oxysporum was cultivated for 24 h at 28 °C after being treated with Ne-FvEO (0.5 mg/mL) and T-FvEO (0.5 mg/mL). Subsequently, the transcriptome and metabolome of hyphae were examined by MetWare Biological Science and Technology Co. Ltd. (Wuhan, China). The differentially expressed genes (DEGs) were identified using the DESeq2 R package with padj <0.05 and |log 2 (fold change)| ≥ 1.0. The differentially accumulated metabolites (DAMs) were screened with variable importance in the projection (VIP) ≥ 1.0, fold change (FC) ≥ 2.0 or FC ≤ 0.5 and Pvalue <0.05. Significant enrichment pathways for DEGs and DAMs were identified using the Kyoto Encyclopedia of Genes and Genomes (KEGG) database.

2.9. RNA extraction and quantitative real-time (qRT)-PCR

To verify the reliability of the transcriptome data, we selected 10 key differential genes for qPCR analysis. Total RNA was isolated with Trizol separation reagent, and the first cDNA was synthesized from 1 g total RNA by Transgene Biotech. The qRT-RCR trial was divided into 3 biological replicates and 3 technical replicates. The primers were shown in Table S1, with QTUB as the internal reference gene.

2.10. In vivo experiments

The roots of *P. notoginseng* were cut into small pieces of approximately 0.5 cm. They were placed on water agar after disinfecting with alcohol and sodium hypochlorite. A mycelium mass with a diameter of 5 mm was placed in the center of root tissue as a positive control, and 5 μL of Ne-FvEO (0.5 mg/mL) or sterile water was added to the mycelium mass as a treatment group.

Healthy annual *P. notoginseng* plants were injected with 10 mL of 0.5 mg/mL Ne-FvEO after being inoculated for 24 h with a concentration of 1×10^5 spore suspension. To study the control effect of Ne-FvEO against *F. oxysporum*, the total chlorophyll content, disease incidence, and disease index of *P. notoginseng* were assessed 45 days after inoculation. The disease incidence and index of plant were caculted according to earlier publications [22].

2.11. Statistical analysis

Statistical Package for Social Science (SPSS, version 19.0 for Windows) was used for data analysis. Analysis of the difference in treatment was done using one-way analysis of variance (ANOVA) and Tukey's test. The difference between the two groups was investigated using an independent *t*-test. $P < 0.05$ was used in this investigation to define a meaningful difference. All experiments in this study were repeated three times.

3. Results

3.1. Phase diagram of nanoemulsions and measurement of particle size and conductivity detection

In the pseudoternary phase diagram, only the nanoemulsion region was drawn (as shown in Fig. S1), and the results showed that when Km = 2, the area of the three-phase diagram formed by Ne-FvEO was the largest, and the optimal Km value was determined. The production flow charts of Ne-FvEO and T-FvEO were shown in Figs. S2A and S2B, respectively.

The actual size and shape of Ne-FvEO and T-FvEO were characterized by TEM.

Both emulsions appear as uniform black droplets without aggregation or coalescence (Figs. S3A and B). The results of the laser particle size analyzer (Figs. S3C and D) showed that the average particle size of T-FvEO was 962.69 ± 253.10 nm and that of Ne-FvEO was 28.730 ± 1.372 nm.

3.2. Analysis of Ne-FvEO stability

The stability of Ne-FvEO at different salt concentrations, temperatures, pH, and rotational speeds was evaluated based on changes in transmittance (Figs. S4A–D). The results show that temperature and salt concentration have little influence on the light transmittance of Ne-FvEO, but pH has some influence. After the nanoemulsion was stored at room temperature and −4 °C for 30 days, no drug precipitation and flocculation were observed. In order to avoid particle aggregation, static delamination and demulsification during storage, processing and

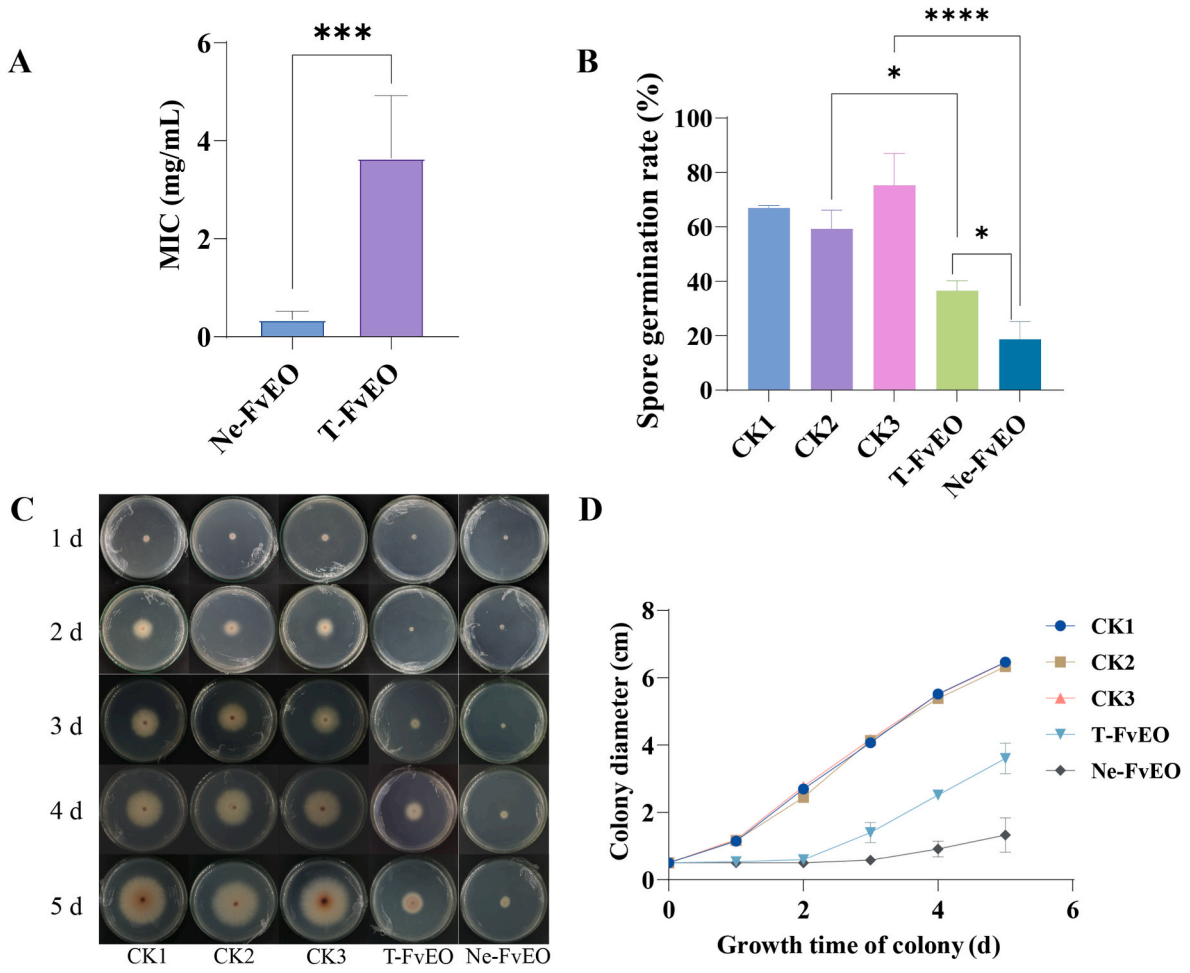

Fig. 2. Effects of different treatment conditions on the growth of *F. oxysporum*. (A) Histogram of spore germination of *F. oxysporum*. CK1: sterile water; CK2: 1/1000 Tween-80 and 20/1000 DMSO; CK3: 100 % ethanol and 1/1000 Tween-80. (B) The MIC of Ne-FvEO and T-FvEO against *F. oxysporum*. (C, D) Effects of different treatment conditions on hyphal growth of *F. oxysporum*. The data represent the means±SEs of three independent replicates, and the significant differences between the treatments and the controls were analyzed by Student's *t*-test (*$p < 0.05$, ****$p < 0.0001$).

transportation, the stability of nanoemulsion was tested by centrifugal acceleration method. The results show that the rotational speed has no effect on the stability of Ne-FvEO. As can be seen from Fig. S4E, there was no significant change in the antifungal activity of Ne-FvEO after different light treatments.

3.3. Analysis of GC–MS results

The chemical compositions of FvEO, Ne-FvEO and T-FvEO were analyzed by GC-MS analysis. As shown in Fig. 1A, the compositions of FvEO and Ne-FvEO are more similar, indicating that Ne-FvEO better preserves the original composition of FvEO. FvEO is mainly composed of terpenes, ethers, ketones and a small amount of phenolics. 29 chemical components of FvEO were identified, and its main components are anethole (40.08 %), estragole (40.74 %), (−)-fenchone (8.94 %) and D-limonene (7.18 %). 27 chemical components of Ne-FvEO were identified, and the main components of Ne-FvEO are anethole (39.99 %), estragole (41.56 %), (−)-fenchone (9.49 %), and D-limonene (6.11 %). 20 chemical components of T-FvEO were identified, and the main components of T-FvEO are anethole (53.43 %) and (−)-fenchone (5.61 %). The three have six chemical components in common: estragole, anethole, α-pinene, β-myrcene, (±)-camphor, and fenchyl acetate (Fig. 1B).

3.4. Results of antifungal activity

As shown in Fig. 2, under all experimental conditions, Ne-FvEO had higher antifungal activity against *F. oxysporum* than T-FvEO. The MIC of Ne-FvEO and T-FvEO for *F. oxysporum* were 0.35 mg/mL and 3.65 mg/mL, respectively (Fig. 2A). The MIC value of Ne-FvEO against *F. oxysporum* was almost ten times that of T-FvEO. As shown in Fig. 2B, C and D, the number of spore germination and the growth of colony were inhibited by Ne-FvEO and T-FvEO. Compared with the control group, the two solvents (CK2 and CK3) did not inhibit the growth of *F. oxysporum* mycelia and conidial germination at all tested concentrations. The results showed that the difference was not caused by the solvent, but by the change in the effective antifungal composition of EO caused by the technology.

3.5. In vivo experiments of P. notoginseng

In this study, 0.5 mg/mL Ne-FvEO was used as the treatment concentration in vivo. Preliminary experimental results showed that Ne-FvEO had a strong inhibitory effect on *F. oxysporum* (Fig. 2). Therefore, to explore whether Ne-FvEO had the same inhibitory effect on *F. oxysporum* after acting on *P. notoginseng*, we inoculated *F. oxysporum* on *P. notoginseng* and treated them with Ne-FvEO. After 6 days of treatment, the lesion area of *P. notoginseng* root slices inoculated with Ne-FvEO (10.92 mm^2) was significantly smaller than that of

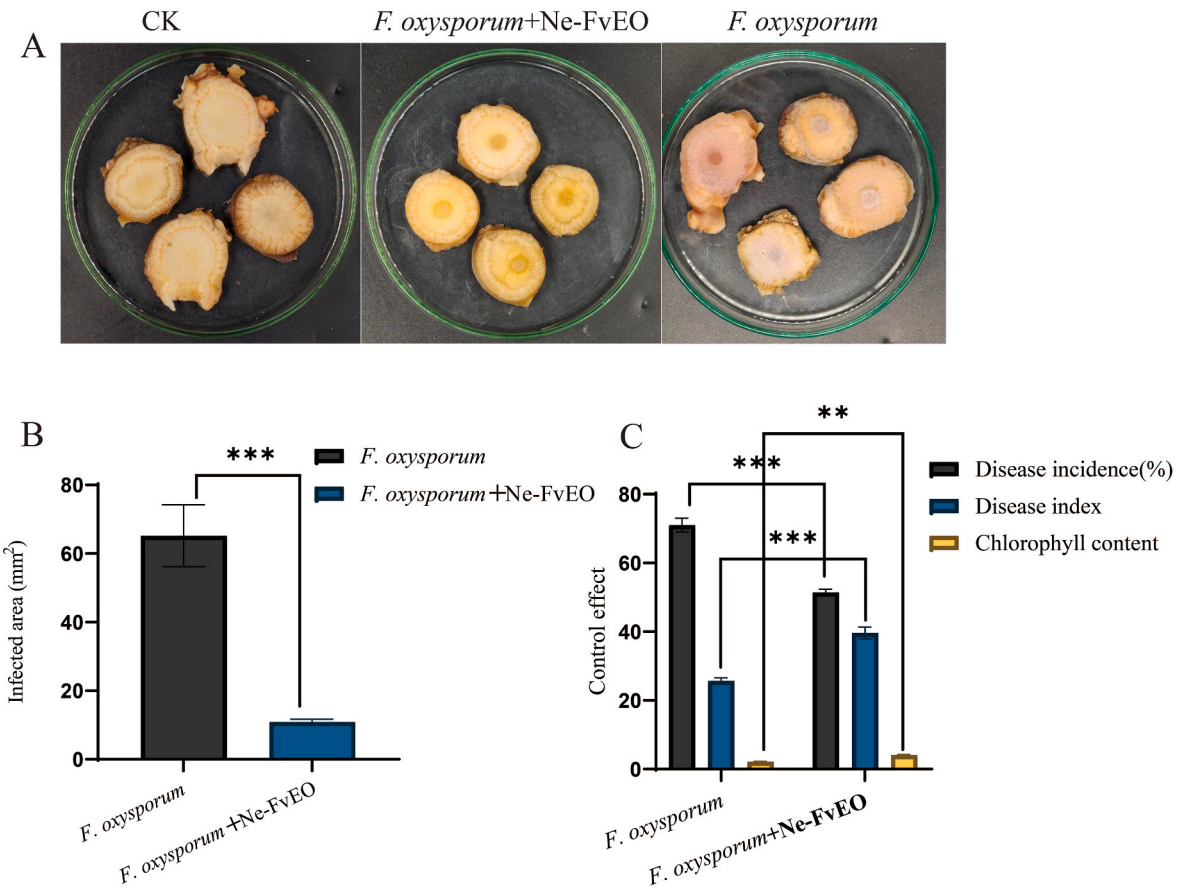

Fig. 3. (A, B) The control effect of Ne-FvEO on isolated roots of *P. notoginseng*. (C) The control effect of Ne-FvEO on root rot of *P. notoginseng* seedlings caused by *F. oxysporum*. (Data are expressed as the mean ± SD of five biological replicates of three replicates. * *, P < 0.01, * * *, P < 0.001).

P. notoginseng root slices inoculated with *F. oxysporum* (61.19 mm^2) alone (Fig. 3A and B). The incidence and disease index of *P. notoginseng* seedlings inoculated with *F. oxysporum* were significantly higher than those of *P. notoginseng* seedlings inoculated with Ne-FvEO. The chlorophyll content of the Ne-FvEO + *F. oxysporum* group was higher than that of the *F. oxysporum* group (Fig. 3C). The results showed that Ne-FvEO maintained high antifungal activity after application to *P. notoginseng*.

3.6. Transcriptome analysis of *F. oxysporum* treated with Ne-FvEO and T-FvEO

To elucidate the molecular mechanism by which Ne-FvEO and T-FvEO inhibit *F. oxysporum*, the overall gene expression of Ne-FvEO, T-FvEO, and sterile water-treated *F. oxysporum* was analyzed. The GO annotation analysis of DEGs showed a total of 6, 10 and 4 GO items related to molecular function, biological processes and cellular components, respectively (Fig. 4A). DEGs related to molecular function are mainly involved in catalytic activity and binding. The DEGs associated with biological processes involved mostly metabolic processes and cellular processes. In terms of cell components, the proportion of DEGs related to membrane components and cell anatomical entities was the highest, followed by organelles. GO analysis showed that Ne-FvEO and T-FvEO inhibited *F. oxysporum* by influencing their catalytic activity, metabolic process, membrane composition and other organelles.

A Venn diagram showed that Ne-FvEO and T-FvEO had 4000 common DEGs (Fig. 4B). The top 20 KEGG enrichment pathways of DEGs in the two comparison groups were analyzed (Fig. 4C and D). In the CK vs. Ne-FvEO and CK vs. T-FvEO samples, the most important pathways were eukaryotic ribosomal biogenesis, endoplasmic reticulum protein processing, valeric acid, leucine, and isoleucine degradation, peroxisome, and endocytosis. In CK vs. Ne-FvEO, the specific pathways included fatty acid metabolism, fatty acid degradation, and butyric acid metabolism. In CK vs. T-FvEO, the most abundant pathway involves carbon metabolism, oxidative phosphorylation, and the TCA cycle. These results suggest that Ne-FvEO and T-FvEO have significant effects on the gene expression of *F. oxysporum*, which altered many metabolic pathways of *F. oxysporum*, such as the biosynthesis of secondary metabolites, metabolism of amino acids and carbohydrates, and transcriptional translation.

3.7. Metabolome analysis of *F. oxysporum* treated with Ne-FvEO and T-FvEO

After treatment with CK, Ne-FvEO and T-FvEO, PCA was performed on the metabolites. PCA results showed obvious differences among the three different treatment groups, highlighting the obvious metabolic differences among different treatment groups (Fig. S5A). The cluster heatmaps of metabolites also showed similarities between biological repeats and differences between treatment groups (Fig. S5B). Volcanic maps show upregulated, downregulated, or unchanged DAMs between CK vs. Ne-FvEO and CK vs. T-FvEO (Figs. S5C and D). The venn map of the DAMs shows differential accumulation of metabolites between the three groups of samples, with 141 metabolites jointly upregulated and 56 jointly downregulated in the metabolites (Figs. S5E and F).

KEGG pathway enrichment analysis of DAMs (Fig. 4E and F) showed that purine metabolism, nucleotide metabolism, butyric acid metabolism, and lysine degradation were coenriched in the CK vs. Ne-FvEO and CK vs. T-FvEO groups, and linolic acid metabolism and tyrosine metabolism were significantly enriched in the CK vs. Ne-FvEO group. Carbon metabolism and glycine metabolism pathways were significantly enriched in the CK vs. T-FvEO group. These results indicated that Ne-

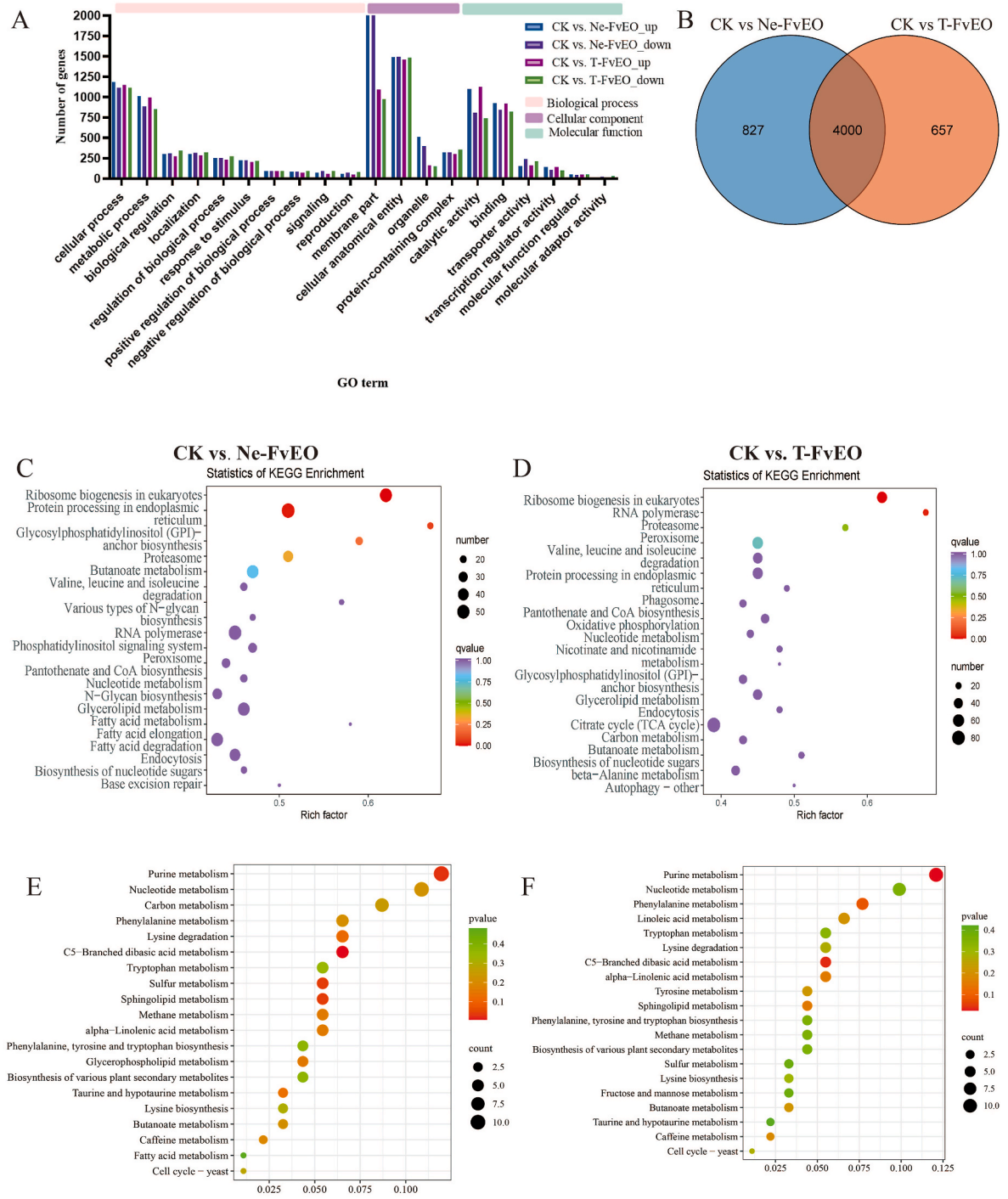

Fig. 4. DEGs presented as a histogram based on the GO classification. (A) Venn diagram (B) and KEGG enrichment (C, D). (E, F) The top 20 enriched KEGG pathways of DAMs. The y-axis displays the KEGG pathway, the x-axis shows the degree of enrichment, and the size of the circle indicates the number of enriched genes or metabolites.

FvEO and T-FvEO had an effect on the metabolites of *F. oxysporum*, which changed many metabolic pathways of *F. oxysporum*, such as purine metabolism, nucleotide metabolism and a series of amino acid metabolism.

3.8. Integration analysis of transcriptomic and metabolic datasets

To further investigate the mechanism by which Ne-FvEO and T-FvEO inhibit *F. oxysporum*, correlations between the transcriptome and metabolome were analyzed in the three groups of samples. Correlation network diagrams show strong correlations between many genes and metabolites. These enrichment pathways were mainly related to the cell wall, cell membrane, energy and nutrient metabolism, and genetics, such as carbon metabolism, amino acid biosynthesis, sphingolipid metabolism, and purine metabolism (Figs. S6A–E).

Based on the results of combined transcriptome and metabolome analysis, four enriched pathways (citrate cycle, lysine degradation, alanine, aspartate and glutamate metabolism, and butanoate metabolism) were chosen to construct the metabolic network of related pathways (Fig. S7). The outcomes demonstrated that Ne-FvEO and T-

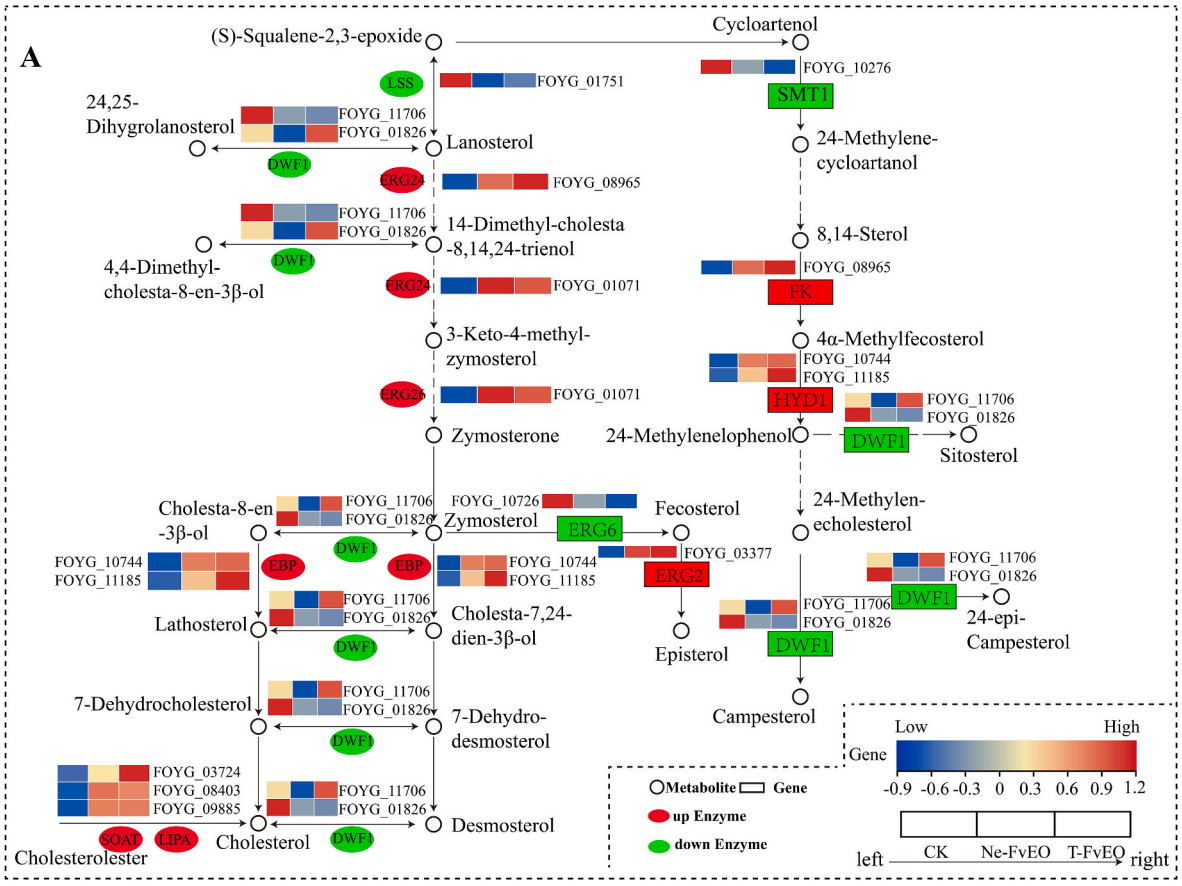

Fig. 5. Metabolic network map of DEGs and DAM sterol biosynthesis pathways in the Ne-FvEO treatment group. The circles represent the metabolites. The rectangles represent the genes (red indicates upregulation; blue denotes downregulation). The ovals represent enzymes (red denotes upregulation; green denotes downregulation).

FvEO treatment had an impact on the metabolites and genes in the four pathways. Several genes were activated in the TCA cycle, which was followed by the buildup of oxyglutaric acid. As shown in Fig. 5, the expression levels of related enzymes and their genes in the steroid biosynthesis pathway were down-regulated, and the down-regulated level in the Ne-FvEO treated group was higher than those in the T-FvEO treated group. In fungi, sterol is essential for membrane structure and motility. The adaptability of fungal membrane to environmental conditions is mainly related to the change of sterol level. These results indicated that Ne-FvEO may had a greater destructive effect on the cell membrane of *F. oxysporum*, and therefore had a stronger antifungal effect.

3.9. Validation of key genes by qPCR

To verify the accuracy of RNA-seq data, 10 genes were selected for qRT-PCR analysis. The 10 genes include four genes (*FOYG_01066*, *FOYG_05437*, *FOYG_02901*, *FOYG_14,766*) involved in energy metabolism, and four genes (*FOYG_06609*, *FOYG_02825*, *FOYG_04335*, *FOYG_01591*) involved in amino acid metabolism, and two genes (*FOYG_10,744*, *FOYG_10,276*) involved in sterol biosynthesis. The results of qPCR were basically consistent with the expression levels recorded by RNA-seq (Fig. S8), which proved the reliability of the data.

4. Discussion

Many plant EO nanoemulsions, such as Peppermint EO nanoemulsion and Laurel EO nanoemulsion, showed better antimicrobial activity against microorganisms [23,24]. One study showed that an optimal garlic oil nanoemulsion had better antifungal activity against *Penicillium italicum* than pure garlic oil. In addition, after the preparation of nanoemulsion, the MIC of garlic oil changed from 3.7 % to 0.01265 %, and the bioavailability increased by approximately 300 times. In our study, Ne-FvEO had higher antifungal activity against *F. oxysporum* than T-FvEO under all experimental conditions (Fig. 2). Therefore, the preparation of EO into nanoemulsion has the potential to improve their antimicrobial activity [25].

Typically, the antimicrobial potential of EO nanoemulsions depends on the phytochemical composition and fungal type. Additionally, droplet size, viscosity, and emulsion formulation are major influences of nanoparticle properties [26,27]. Nanoemulsions improve the passive absorption mechanisms of cells due to their small droplet size, which reduces mass transfer resistance and increases antifungal capacity [28,29]. Compared with T-FvEO, the particle size of Ne-FvEO was reduced by about 34 times, and the MIC showed that the antifungal activity was increased by 10 times. Ne-FvEO showed good stability under different test conditions (Fig. 2, S4). Terpenoids, phenols, and aldehydes are the main chemical components with antifungal effect, and their concentration and chemical composition have important effects on the antifungal activity of EOs [30,31]. These differences in the results of EO antifungal activity may be related to changes in the levels of major and minor components as well as synergistic effects among all components. This study found that EO mainly contained terpenes, ethers, ketones and a small amount of phenolic aldehyde, while T-FvEO did not contain estragole, (−)-fenchone, or D-limonene (Fig. 1). Studies have demonstrated that the strong antifungal properties of estragole, (−)-fenchone, and D-limonene [32–34]. Therefore, the smaller particle size, stronger stability and higher content of antifungal chemical components are the

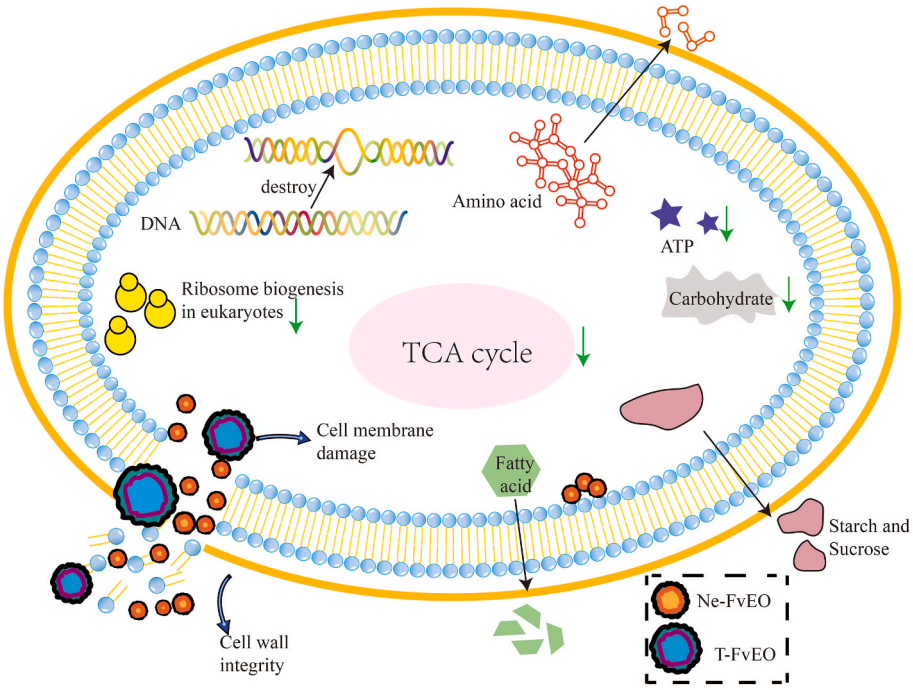

Fig. 6. Hypothetical diagram of the mechanism of action of Ne-FvEO and T-FvEO against *F. oxysporum*.

reasons why Ne-FvEO has stronger antifungal effect than T-FvEO.

Cell walls and cell membranes have been proposed as targets for EOs [35–37]. Most dynamic structure of cell wall is composed of chitin, glucan, mannan and glycoprotein [38]. The enzyme known as chitin synthetase (CHS) is crucial for the synthesis of chitin and is involved in the growth and physiology of fungus [39]. Numerous lipids, such as glycerophospholipids, sphingolipids, and sterols, are abundant in the membranes of certain fungi [40]. The degradation of membrane function and structure caused by ergosterol depletion prevents the growth of fungi [41]. In this study, Ne-FvEO and T-FvEO treatments reduced the expression of genes involved in sterol biosynthesis pathways and cell wall chitin metabolism (Fig. 6, S6E).

Over ninety-of the energy needed by eukaryotic cells is generated by the tricarboxylic acid cycle (TCA cycle) [42]. Furthermore, it has been demonstrated that RocG, which is a crucial enzyme in the breakdown of glutamate, can catalyzes the synthesis of 2-oxoglutarate, which is a component of the TCA cycle and is required for spore germination [43]. The changes of genes and enzymes after Ne-FvEO and T-FvEO treatment were shown in the TCA pathway network diagram. The accumulation of metabolite 2-oxoglutaric acid was decreased, and the decrease was greater after Ne-FvEO treatment (Fig. S7). This may be one of the reasons why Ne-FvEO is more significant in inhibiting fungal growth.

The production of proteins that promote cell growth is based on ribosomes, the formation of which is necessary for both cell growth and proliferation [44]. The biosynthesis and catabolism of purine nucleotides are crucial for the growth and development of fungi [45]. In this study, eukaryotic ribosome biosynthesis and purine metabolism pathways were significantly enriched in both the transcriptome and metabolome (Fig. 4C–F). These results indicated that both treatments could affect the ribosome biosynthesis and purine metabolism of *F. oxysporum*, thereby exerting antifungal effects. Transcriptomic and metabolomic analysis showed that Ne-FvEO and T-FvEO treated groups entered *F. oxysporum* cells by destroying cell walls and cell membranes. They also affect ribosome biosynthesis, purine metabolism and energy metabolism of *F. oxysporum*, ultimately leading to their inhibition.

Declaration of competing interest

The authors declare no competing financial interest.

CRediT authorship contribution statement

Hongyan Nie: Methodology, Software, Writing – original draft. Hongxin Liao: Conceptualization, Methodology, Software. Jinrui Wen: Conceptualization, Methodology. Cuiqiong Ling: Investigation. Liyan Zhang: Investigation. Furong Xu: Data curation. Xian Dong: Writing – review & editing, Funding acquisition.

Acknowledgements

This work was funded by the National Natural Science Foundation of China (82060683), Yunnan Provincial Science and Technology Plan-Basic Research Project (202301AW070008), Wang Yuan Chao Expert Workstation in Yunnan Province (202305AF150018), Yunnan Provincial Science and Technology Department-Applied Basic Research Joint Special Funds of Yunnan University of Traditional Chinese Medicine (202101AZ070001-047), Yunnan Key Laboratory of Southern Medicinal Utilization, Yunnan University of Chinese Medicine (202105AG070012XS23011).

Appendix A. Supplementary data

Supplementary data to this article can be found online at https://doi.org/10.1016/j.jgr.2023.12.002.

References

[1] Wang T, Guo R, Zhou G, Zhou X, Kou Z, Sui F, et al. Traditional uses, botany, phytochemistry, pharmacology and toxicology of *Panax notoginseng* (Burk.) F.H. Chen: a review. J Ethnopharmacol 2016;188:234–58.

[2] Guo HB, Cui XM, An N, Cai GP. Sanchi *ginseng* (*Panax notoginseng* (Burkill) F. H. Chen) in China: distribution, cultivation and variations. Genet Resour Crop Evol 2010;57:453–60.

[3] Miao Z, Li S, Liu X, Chen Y, Li Y, Wang Y, et al. The causal microorganisms of *Panax notoginseng* root rot disease. Chin Agric Sci 2006;39:1371–8.

[4] Kooti W, Moradi M, Ali-Akbari S, Sharafi-Ahvazi N, Ashtary-Larky D. Therapeutic and pharmacological potential of *Foeniculum vulgare* Mill: a review. J HerbMed Pharmacol 2015;4:1–9.
[5] Abed NE, Kaabi B, Smaali MI, Chabbouh M, Habibi K, Mejri M, et al. Chemical composition, antioxidant and antimicrobial activities of *Thymus capitata* essential oil with its preservative effect against *Listeria monocytogenes* inoculated in minced beef meat. Evid-based Compl Alt 2014:152487.
[6] Ozogul Y, Boğa EK, Akyol I, Durmus M, Ucar Y, Regenstein JM, Köşker AR. Antimicrobial activity of thyme essential oil nanoemulsions on spoilage bacteria of fish and food-borne pathogens. Food Biosci 2020;36.
[7] Cui H, Zhao C, Lin L. The specific antibacterial activity of liposome-encapsulated clove oil and its application in tofu. Food Control 2015;56:128–34.
[8] Ju J, Xie Y, Guo Y, Cheng Y, Qian H, Yao W. Application of edible coating with essential oil in food preservation. Crit Rev Food Sci Nutr 2019;59:2467–80.
[9] Ju J, Chen X, Xie Y, Yu H, Yao W. Application of essential oil as a sustained release preparation in food packaging. Trends Food Sci Technol 2019;92:22–32.
[10] Zhang W, Cao X, Liu SQ. Aroma modulation of vegetable oils-A review. Crit Rev Food Sci Nutr 2020;60:1538–51.
[11] Badgujar SB, Patel VV, Bandivdekar AH. *Foeniculum vulgare* Mill: a review of its botany, phytochemistry, pharmacology, contemporary application, and toxicology. BioMed Res Int 2014;4:842674.
[12] Singh G, Maurya S, Lampasona M, Catalan C. Chemical constituents, antifungal and antioxidative potential of *Foeniculum vulgare* volatile oil and its acetone extract. Food Control 2006;17:745–52.
[13] Soylu S, Yigitbas H, Soylu EM, Kurt S. Antifungal effects of essential oils from oregano and fennel on *Sclerotinia sclerotiorum*. J Appl Microbiol 2010;103: 1021–30.
[14] Prakash B, Kujur A, Yadav A, Kumar A, Singh PP, Dubey NK. Nanoencapsulation: an efficient technology to boost the antimicrobial potential of plant essential oils in food system. Food Control 2018:1–11.
[15] Chaudhari AK, Dwivedy AK, Singh VK, Das S, Singh A, Dubey NK. Essential oils and their bioactive compounds as green preservatives against fungal and mycotoxin contamination of food commodities with special reference to their nanoencapsulation. Environ Sci Pollut Res 2019;26(25):25414–31.
[16] Yang R, Miao J, Shen Y, Cai N, Chen J. Antifungal effect of Cinnamaldehyde, Eugenol and Carvacrol nanoemulsion against *Penicillium digitatum* and application in postharvest preservation of Citrus fruit. LWT–Food Sci Technol 2021;141: 110924.
[17] Das S, Singh VK, Dwivedy AK, Chaudhari AK, Upadhyay N, Singh A, et al. Fabrication, characterization and practical efficacy of *Myristica fragrans* essential oil nanoemulsion delivery system against postharvest biodeterioration. Ecotoxicol Environ Saf 2020;189:110000.
[18] Balouiri M, Sadiki M, Ibnsouda SK. Methods for in vitro evaluating antimicrobial activity: a review. J Pharm Anal 2016;6:71–9.
[19] Sindhu F, Carpenter L, Seers K. Development of a tool to rate the quality assessment of randomized controlled trials using a Delphi technique. J Adv Nurs 2010;25:1262–8.
[20] Xu Y, Wei J, Wei Y, Han P, Dai K, Zou X, et al. Tea tree oil controls brown rot in peaches by damaging the cell membrane of *Monilinia fructicola*. Postharvest Biol Technol 2021:175.
[21] Ma YN, Chen CJ, Li QQ, Wang W, Xu FR, Cheng YX, et al. Fungicidal activity of essential oils from *Cinnamomum cassia* against the pathogenic fungi of *Panax notoginseng* diseases. Chem Biodivers 2019;16:e1900416.
[22] Chen CJ, Li QQ, Ma YN, Wang W, Cheng YX, Xu FR, et al. Antifungal effect of essential oils from five kinds of Rutaceae plants - avoiding pesticide residue and resistance. Chem Biodivers 2019;16:e1800688.
[23] Liu Q, Gao Y, Fu X, Chen W, Chen Y. Preparation of peppermint oil nanoemulsions: investigation of stability, antibacterial mechanism and apoptosis eects. Colloids Surf, B 2021;201:111626.
[24] Özogul Y, El Abed N, Özogul F. Antimicrobial effect of laurel essential oil nanoemulsion on food-borne pathogens and fish spoilage bacteria. Food Chem 2022;368:130831.
[25] Long Y, Huang W, Wang Q, Yang G. Green synthesis of garlic oil nanoemulsion using ultrasonication technique and its mechanism of antifungal action against *Penicillium italicum*. Ultrason Sonochem 2020;64:104970.
[26] Yazgan H, Ozogul Y, Boga EK. Antimicrobial influence of nanoemulsified lemon essential oil and pure lemon essential oil on food-borne pathogens and fish spoilage bacteria. Int J Food Microbiol 2019;306:108266.
[27] Zogul Y, Kuley E, Akyol I, Durmu M, Kosker AR. Antimicrobial activity of thyme essential oil nanoemulsions on spoilage bacteria of fish and food-borne pathogens. Food Biosci 2020;36.
[28] Prakash A, Vadivel V, Rubini D, Nithyanand P. Antibacterial and antibiofilm activities of linalool nanoemulsions against *Salmonella Typhimurium*. Food Biosci 2019;28:57–65.
[29] Patrignani F, Siroli L, Braschi G, Lanciotti R. Combined use of natural antimicrobial based nanoemulsions and ultra high pressure homogenization to increase safety and shelf-life of apple juice. Food Control 2020;111:107051.
[30] Seow YX, Yeo CR, Chung HL, Yuk HG. Plant essential oils as active antimicrobial agents. Crit Rev Food Sci Nutr 2014;54:625–44.
[31] Reyes-Jurado F, Navarro-Cruz AR, Ochoa-Velasco CE, Palou E, López-Malo A, Ávila-Sosa R. Essential oils in vapor phase as alternative antimicrobials: a review. Crit Rev Food Sci Nutr 2020;60(10):1641–50.
[32] Andrade TC, De Lima SG, Freitas RM, Rocha MS, Islam T, Da Silva TG, et al. Isolation, characterization and evaluation of antimicrobial and cytotoxic activity of estragole, obtained from the essential oil of *Croton zehntneri* (Euphorbiaceae). An Acad Bras Cienc 2015;87:173–82.
[33] Singh S, Gupta P, Gupta J. Virtual structural similarity elucidates bioactivity of Fenchone: a phytochemical enriched in Fennel essential oil. Curr Drug Discov Technol 2020;17:619–30.
[34] Oliveira RC, Carvajal-Moreno M, Mercado-Ruaro P, Rojo-Callejas F, Correa B. Essential oils trigger an antifungal and anti-aflatoxigenic effect on *Aspergillus flavus* via the induction of apoptosis-like cell death and gene regulation. Food Control 2019;110:107038.
[35] Bakkali F, Averbeck S, Averbeck D, Idaomar M. Biological effects of essential oils-a review. Food Chem Toxicol 2008;46:446–75.
[36] Shao X, Cheng S, Wang H, Yu D, Mungai C. The possible mechanism of antifungal action of tea tree oil on *Botrytis cinerea*. J Appl Microbiol 2013;114:1642–9.
[37] Zhou T, Wang X, Ye B, Shi L, Bai X, Lai T. Effects of essential oil decanal on growth and transcriptome of the postharvest fungal pathogen *Penicillium expansum*. Postharvest Biol Technol 2018;145:203–12.
[38] Sant DG, Tupe SG, Ramana CV, Deshpande MV. Fungal cell membrane-promising drug target for antifungal therapy. J Appl Microbiol 2016:121.
[39] Marie-Christine S, Perino C, Piffeteau A, Choquer M, Vidal-Cros A. *Botrytis cinerea* virulence is drastically reduced after disruption of chitin synthase class III gene (Bcchs3a). Cell Microbiol 2010;8:1310–21.
[40] Bowman SM, Free SJ. The structure and synthesis of the fungal cell wall. Bioessays 2006;28:799–808.
[41] Han S, Chen J, Zhao Y, Cai H, Guo C. *Bacillus subtilis* HSY21 can reduce soybean root rot and inhibit the expression of genes related to the pathogenicity of *Fusarium oxysporum*. Pestic Biochem Physiol 2021;178:104916.
[42] Ju J, Xie Y, Yu H, Guo Y, Cheng Y, Zhang R, et al. Synergistic inhibition effect of citral and eugenol against *Aspergillus niger* and their application in bread preservation. Food Chem 2020;310:125974.
[43] Rao L, Zhou B, Serruya R, Moussaieff A, Sinai L, Ben-Yehuda S. Glutamate catabolism during sporulation determines the success of the future spore germination. iScience 2022;25:105242.
[44] Ameismeier M, Zemp I, Heuvel J, Thoms M, Beckmann R. Structural basis for the final steps of human 40S ribosome maturation. Nature 2020;587:1–5.
[45] Ljungdahl PO, Daignan-Fornier B. Regulation of amino acid, nucleotide, and phosphate metabolism in *Saccharomyces cerevisiae*. Genetics 2012;190:885–929.